IEEE INSTRUMENTATION & MEASUREMENT SOCIETY

Received 14 December 2022; revised 4 February 2023; accepted 7 February 2023. Date of publication 28 February 2023; date of current version 20 March 2023.
The review of this article was arranged by Associate Editor Alessandro M. Ferrero.

Digital Object Identifier 10.1109/OJIM.2023.3250280

Refined Modeling and Compensation of Current Transformers Behavior for Line Parameters Estimation Based on Synchronized Measurements

CHRISTIAN LAURANO [1] (Member, IEEE), PAOLO ATTILIO PEGORARO [2] (Senior Member, IEEE), CARLO SITZIA [2] (Graduate Student Member, IEEE), ANTONIO VINCENZO SOLINAS [2] (Member, IEEE), SARA SULIS [2] (Senior Member, IEEE), AND SERGIO TOSCANI [2] (Senior Member, IEEE)

[1]Dipartimento di Elettronica, Informazione e Bioingegneria, Politecnico di Milano, 20156 Milan, Italy

[2]Department of Electrical and Electronic Engineering, University of Cagliari, 09123 Cagliari, Italy

CORRESPONDING AUTHOR: S. SULIS (e-mail: sara.sulis@unica.it)

The work of Paolo Attilio Pegoraro was supported in part by the Fondazione di Sardegna for the Research Project "IQSS, Information Quality Aware and Secure Sensor Networks for Smart Cities," year 2020.

ABSTRACT Nowadays, in modern management and control applications, line parameters need to be known more accurately than in the past to achieve a reliable operation of the distribution grids. Phasor measurement units (PMUs) may improve line parameter estimation processes, but the accuracy of the result is affected by all the elements of the PMU-based measurement chain, in particular by the instrument transformers. Current transformers (CTs) are nonlinear and, therefore, their behavior is not easily described: their models cannot be straightforwardly included in the estimation problem. In this regard, this article refines modeling and compensation of CT systematic errors in line parameter estimation processes, based on different methods to describe the transformer behavior under various operating conditions. As the main result, the systematic errors of CTs are remarkably identified and mitigated. Moreover, the estimation of shunt susceptance values is significantly improved.

INDEX TERMS Current transformers (CTs), instrument transformers (ITs), line parameters, power distribution systems (DSs), random errors, synchrophasor measurements, systematic errors, voltage transformers (VTs).

I. INTRODUCTION

IN THE evolving scenario of distribution systems (DSs), new monitoring and management tools are emerging. Each of them should rely on an accurate model of the network itself, in terms of topology [1], loads, generators, etc. Many applications proposed for DS management assume indeed known line parameters. However, such parameters can be significantly different with respect to those available in DS operators (DSOs) databases, which are often derived from the nominal line geometry and length, as well as from the datasheets provided by the cable manufacturers. This leads to a mismatch that can reach tens of percent [2].

An online measurement of line parameters would be of great help in improving the network model and, in this regard, phasor measurement units (PMUs) might provide highly accurate inputs for this task. Therefore, their synchronized set of measurements, reported at the given time instants (Universal Coordinated Time, UTC, time reference), allow defining a line parameter estimation problem through time-aligned phasors. In addition, PMUs feature high reporting rate (RR, tens to hundreds of measurements per second) corresponding to frequent snapshots of the monitored quantities [3].

PMU measurements have already been exploited to estimate transmission network line parameters, but the interest is emerging also for refining DS models [4]. In the literature, various methodologies have been presented for the estimation of the line parameters of transmission grids, see for instance [5], [6], [7]. Fewer papers dealt with the estimation of DS line parameters (e.g., [8], [9], [10], [11], and [12]). However,

the description of the errors occurring in the measurement process does not typically consider all the significant sources of uncertainty. In fact, [8], [9], and [10] only consider the error contribution due to PMUs. In [11] and [12], the entire measurement chain is taken into account but assuming that errors are only random. In [13], the limit of neglecting the error contribution of instrument transformers (ITs) in the estimation model is discussed. ITs are typically responsible for the largest uncertainty contributions [14], but they are often neglected or just considered through purely random error sources.

It is possible to say that in the presence of IT systematic errors, a direct computation of line parameters from synchrophasor measurements is practically unfeasible.

In [15], a method was proposed to estimate line parameters in DSs together with systematic errors introduced by ITs [16]. The method is based on PMU measurements at both ends of each line and exploits prior information about IT uncertainty. In [17], the method has been extended to include also shunt parameters among the estimates, and it has been tested in the presence of distributed generation (DG). However, the method needs to be validated under more realistic conditions. More specifically, the numerical simulations performed in [15] assume that voltage transformers (VTs) and current transformers (CTs) introduce a systematic ratio error and phase displacement [16]. Their values have been randomly extracted from uniform distributions complying with the corresponding accuracy class, supposed to be uncorrelated with the value of the measurand: in the absence of further information about the metrological behavior of ITs, that is the only admissible choice.

As far as VTs, this assumption is rather reasonable, thanks to the fact that during regular operation, node voltages are rather close to their rated values [18]. In fact, the accuracy class for measuring VTs (both conventional and low-power) prescribes maximum ratio and phase errors that do not depend on the primary voltage magnitude, which may vary between 80% and 120% of the rated value [19], [20].

When considering CTs, the situation is rather different, since the primary current may vary over a broad range. For this reason, as well as for the presence of weak nonlinear effects, assuming that CTs introduce constant ratio and phase errors does not represent, in general, a good approximation [21], [22]. As a matter of fact, considering a given accuracy class for measuring CTs, the relevant standards [23] and [24] allow significantly larger ratio and phase errors in the lowest part of the measurement range.

A deeper study about the behavior of CTs permits a detailed representation of their uncertainty contributions in numerical simulations, thus enabling a better analysis about their impact on the estimates. In this respect, Sitzia et al. [25] considered the nonlinear behavior of CTs through an equivalent circuit. Results show that the accuracy of the measured series parameters is weakly affected, while that of shunt parameters is significantly degraded.

This article, representing the technical extension of [25], proposes a further evolution aimed at overcoming this limitation. Experimental tests have been carried out on CTs from different manufacturers in order to assess their metrological performances. Obtained data have been first used for representing CT errors in numerical simulations, following the same approach adopted in [21] and [22]. Moreover, these data have been also exploited to define simplified parametric models aimed at capturing the basic features of their behavior, in particular the relationship between error values and current magnitude. Finally, the approach [17] has been modified to include the parameters of these elementary CT models in the vector of the estimates. The improved algorithm can thus embed most part of the systematic effects due to CTs: this enables a better reconstruction of line currents and a more accurate measurement of the line parameters, as highlighted by the obtained results.

II. MODELING CT ERRORS

As pointed out during the introduction, the first step that can help improving estimation algorithms, like for example [17], is investigating the metrological behavior of CTs that, as a result of the combination between core nonlinearity and wide measurement range, is not well represented by constant ratio error η and phase displacement (or phase error) ψ [16]. Both experience and mathematical considerations on the CT model confirm that its behavior at the fundamental is barely affected by the presence of harmonics [21], [22], [26]. For this reason, neglecting other influence quantities, η and ψ can be considered as functions of the sole fundamental primary current magnitude I.

According to this simplification, the relationships between η, ψ, and I at 50-Hz frequency have been measured on three different types of class 0.5 CTs operating at rated burden (10 VA with 5-A nominal secondary current). They feature a multitap primary winding that allows setting the nominal primary current. All the CTs have been connected to obtain a rated primary current value $I^0 = 50$ A, but it is worth highlighting that virtually the same behavior would have been observed in the other configurations. In fact, such behavior depends on core magnetization and, thus, the actual input is the primary magnetomotive force, which just depends on I/I^0. For each CT type, two samples have been characterized in order to have an idea about the spread of their performances. Tests have been carried out through the experimental setup reported in Fig. 1.

The primary winding of the CT under test is supplied by means of an AETechron 7548 industrial power amplifier, whose maximum current output capability is increased through a transformer. Primary and secondary currents of the CT have been measured by means of calibrated coaxial shunts (100 and 10-A nominal currents, respectively). Since the resulting voltage signals are too small for being properly acquired, their output terminals have been connected to calibrated high-linearity Analog Devices AD215BY isolation

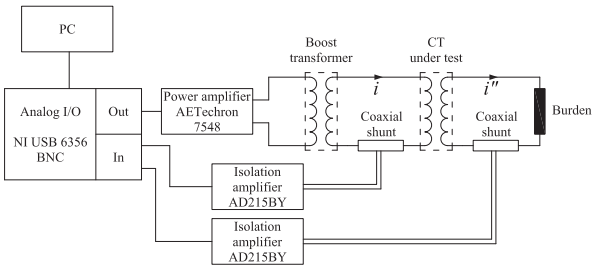

FIGURE 1. Measurement setup for the characterization of CTs.

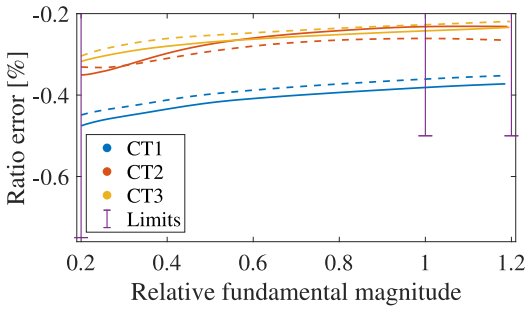

FIGURE 2. Ratio error as a function of I/I^0 for the tested CTs.

amplifiers. It is worth noting that the systematic contributions affecting ratio and phase errors measured on the tested CT just depend on the mismatches between the ratio and phase errors of the two current measurement channels, which are below 10^{-4} and 0.1 mrad. Signal generation, data acquisition, and processing have been managed by a PC connected to a National Instruments NI USB-6356 board with 16-bit resolution, adjustable analog input range, synchronized acquisition, and generation capability.

Tests have been carried out by using the previously described setup to apply 50-Hz sinusoidal currents to the primary winding of the CT under test, with amplitudes ranging from $0.2\,I^0$ to $1.2\,I^0$ with $0.05\,I^0$ step. For each set point, 100 periods of the steady-state primary and secondary current waveforms $i(t)$ and $i''(t)$ have been acquired with 200-kHz rate. Thanks to synchronized acquisition and generation, the corresponding phasors of the primary and secondary side 50-Hz components can be easily extracted without spectral leakage phenomena. Moreover, the impact of noise is heavily mitigated through frequency-domain averaging over the acquired periods [27]. Finally, the trends of the ratio and phase errors as functions of I/I^0 have been obtained. Their noise standard deviations have been quantified and the obtained values can be considered as negligible. Results are reported in Figs. 2 and 3; smoothing splines have been adopted to interpolate between experimental values, solid and dashed lines of the same color denote the two samples of the same CT type.

As expected, in all the cases, error values are well within class 0.5 accuracy limits reported in [23]. Although the trends of each couple of nominally identical samples of the same CT type exhibit some differences, they are clearly similar.

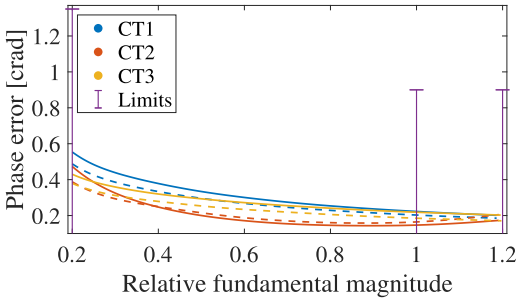

FIGURE 3. Phase error as a function of I/I^0 for the tested CTs.

Moreover, the error curves of different CT types are highly similar. Analyzing the ratio errors $\eta(I/I^0)$, they are all negatively biased (as typically happens for a CT loaded with full burden) and show rather small variations over the investigated current range (about 0.1 crad). Lowest ratio errors are reached near and above the rated current. The sign of the phase errors $\psi(I/I^0)$ reveals that the reconstructed primary current phasor leads the actual one, as a consequence of the inductive nature of the magnetizing current. For all the considered CTs, ψ reaches the smallest magnitude near the rated current (values are between 0.14 and 0.22 crad), but it exhibits a noticeable and almost monotonic increase when moving toward the leftmost part of the graph. In particular, phase error reaches between 0.38 and 0.56 crad at 20% of the nominal value. From a physical point of view, this is due to the typical behavior of ferromagnetic materials at low flux density values, where the magnetizing current is less than proportional to the magnetic flux and, thus, to the primary current. In principle, if one knew the functions $\eta(I/I^0)$ and $\psi(I/I^0)$, it would be possible to accurately compensate for the systematic effects introduced by CTs. However, this demands for a time-consuming and expensive individual characterization of all CTs installed in the grid, which should be also kept updated.

III. ESTIMATION METHOD AND SETTINGS

A. BACKGROUND ON SYNCHROPHASOR ESTIMATION IN THE PRESENCE OF IT SYSTEMATIC ERRORS

This section summarizes the algorithm proposed in [15] to estimate DS line parameters, together with the assumptions that are introduced in order to select its configuration. The constraints of the estimation problem and the associated equations are presented, while highlighting the role of CTs. The measurement model is thus analyzed along with possible weaknesses. As in [15], the discussion considers a single-phase version of the method, while its three-phase formulation can be found in [28].

The monitoring system is composed of PMUs (or distribution PMUs)[1] installed in every node of interest, measuring the voltage and each outgoing branch current. Considering

1. When designed specifically for DSs such instruments are often referred to as distribution PMUs even though up to now no specific standards are available.

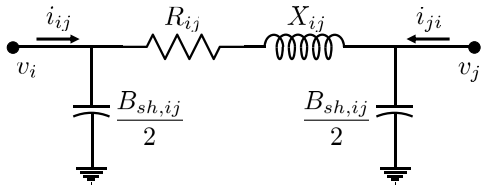

FIGURE 4. π-model for a distribution network branch and its parameters.

a generic branch (i, j), Fig. 4 shows the corresponding π-model, its parameters, and the measured synchrophasors (v_i, v_j, i_{ij}, and i_{ji}). All measurements are performed every T_{RR} seconds (reporting interval) and they share a common timestamp t. The considered line parameters are series resistance R_{ij}, series reactance X_{ij} (so that series impedance is $z_{ij} = R_{ij} + jX_{ij}$) and shunt susceptance $B_{sh,ij}$, evenly split between the sides of the π-model. As typically happens, shunt conductance has been neglected, since during regular operation, its value is negligible with respect to $B_{sh,ij}$.

The estimation algorithm aims at finding the deviations of the line parameters with respect to the nominal values, expressed by

$$\begin{aligned} R_{ij} &= R_{ij}^0\left(1+\gamma_{ij}\right) \\ X_{ij} &= X_{ij}^0\left(1+\beta_{ij}\right) \\ B_{sh,ij} &= B_{sh,ij}^0\left(1+\delta_{ij}\right) \end{aligned} \tag{1}$$

where superscript ^{0} indicates nominal values. The quantities γ_{ij}, β_{ij}, and δ_{ij} are thus the unknown relative deviations and represent the lack of knowledge about parameters.

Unfortunately, the direct estimation of these parameters from Ohm's and Kirchhoff's laws can lead to gross errors produced by the uncertainty introduced by the measurement chain. Systematic errors due to ITs cannot be filtered through averaging and may completely jeopardize the result. For this reason, the estimation algorithm must deal with systematic and random errors in a different way: the former are unknown quantities that can be estimated, while the latter are disturbances that should be rejected thanks to the estimation process. It is therefore important to separate these two contributions in the measurement model. Measurements can thus be expressed as

$$v_h = V_h e^{j\varphi_h} = \left(1+\xi_h^{\mathrm{sys}}+\xi_h^{\mathrm{rnd}}\right)V_h^R e^{j\left(\varphi_h^R+\alpha_h^{\mathrm{sys}}+\alpha_h^{\mathrm{rnd}}\right)} \tag{2}$$

$$i_{ij} = I_{ij} e^{j\theta_{ij}} = \left(1+\eta_{ij}^{\mathrm{sys}}+\eta_{ij}^{\mathrm{rnd}}\right)I_{ij}^R e^{j\left(\theta_{ij}^R+\psi_{ij}^{\mathrm{sys}}+\psi_{ij}^{\mathrm{rnd}}\right)} \tag{3}$$

with $h \in \{i, j\}$ (Fig. 4). Superscript $^{\mathrm{R}}$ indicates the reference value of each quantity. Deviations ξ_h and η_{ij} are the relative errors of voltage and current magnitude measurements, while α_h and ψ_{ij} are the corresponding phase-angle deviations. Superscripts $^{\mathrm{sys}}$ and $^{\mathrm{rnd}}$ denote the systematic or random nature of the contribution, respectively. An expression formally identical to (3) can be written also for i_{ji}. Equations (2) and (3) implicitly assume that the absolute values of ratio errors are $\ll 1$, so that systematic and random contributions can be summed up neglecting the product of the two errors. Following the same approach, while considering that also $|\alpha_h|$ and $|\psi_{ij}|$ are $\ll 1$ (thanks to the typical accuracy of ITs and PMUs), (2) and (3) can be linearized.

The unknowns of the estimation problem can be included in a vector $\mathbf{x}_{ij}$ for each considered branch. In order to find $\mathbf{x}_{ij}$, the constraints given by Kirchhoff's laws are introduced, leading to the following complex-valued equations:

$$v_i^R - v_j^R = \left(R_{ij}+jX_{ij}\right)\left(i_{ij}^R - j\frac{B_{sh,ij}}{2}v_i^R\right) \tag{4}$$

$$i_{ij}^R + i_{ji}^R = j\frac{B_{sh,ij}}{2}\left(v_i^R + v_j^R\right) \tag{5}$$

where (4) is the voltage drop constraint across the branch and (5) is the constraint given by the current balance. Making the reference values explicit from linearized (2) and (3) (and its counterpart for i_{ji}), replacing them into (4) and (5), and using (1), two complex-valued equations in the unknowns are found. They can be linearized, assuming that also $|\gamma_{ij}|$, $|\beta_{ij}|$ and $|\delta_{ij}|$ are $\ll 1$ and keeping only first order expansion terms in the deviations and errors, and then split into their real and imaginary parts. Four real-valued equations in $\mathbf{x}_{ij}$ are then obtained for each branch and timestamp t.

A single timestamp is not enough to define an overdetermined system of equations, since $\mathbf{x}_{ij}$ includes eight systematic errors (two for each measured synchrophasor) and three line parameter deviations (when all the parameters in the π-model are considered). Multiple timestamps $t_1 \ldots t_{N_t}$ are combined to obtain an overdetermined system and perform the estimation from the following problem:

$$\begin{aligned} \mathbf{b}_{ij} &= \left[\mathbf{b}_{ij,t_1} \cdots \mathbf{b}_{ij,t_{N_t}}\right]^{\mathsf{T}} = \mathbf{H}_{ij}\mathbf{x}_{ij} + \boldsymbol{\epsilon}_{ij} \\ &= \mathbf{H}_{ij}\mathbf{x}_{ij} + \mathbf{E}_{ij}\mathbf{e}_{ij} = \mathbf{H}_{ij}\begin{bmatrix} \xi_i^{\mathrm{sys}} \\ \alpha_i^{\mathrm{sys}} \\ \xi_j^{\mathrm{sys}} \\ \alpha_j^{\mathrm{sys}} \\ \eta_{ij}^{\mathrm{sys}} \\ \psi_{ij}^{\mathrm{sys}} \\ \eta_{ji}^{\mathrm{sys}} \\ \psi_{ji}^{\mathrm{sys}} \\ \gamma_{ij} \\ \beta_{ij} \\ \delta_{ij} \end{bmatrix} + \mathbf{E}_{ij}\begin{bmatrix} \mathbf{e}_{ij,t_1} \\ \vdots \\ \mathbf{e}_{ij,t_{N_t}} \end{bmatrix} \end{aligned} \tag{6}$$

where $\mathbf{b}_{ij,t_l}$ is the 4×1 vector corresponding to the known terms in the equations associated with the lth timestamp. Matrix $\mathbf{H}_{ij}$ defines the measurement functions of $\mathbf{x}_{ij}$ and results from the concatenation of the measurement matrices obtained for each timestamp. Matrix $\mathbf{E}_{ij}$ represents the linear transformation from the vector of random errors $\mathbf{e}_{ij}$ to $\boldsymbol{\epsilon}_{ij}$, i.e., the vector of the random errors in the equivalent measurements defined by $\mathbf{b}_{ij}$. Vector $\mathbf{e}_{ij,t_l} = \left[\xi_{i,t_l}^{\mathrm{rnd}}\alpha_{i,t_l}^{\mathrm{rnd}}\xi_{j,t_l}^{\mathrm{rnd}}\alpha_{j,t_l}^{\mathrm{rnd}}\eta_{ij,t_l}^{\mathrm{rnd}}\psi_{ij,t_l}^{\mathrm{rnd}}\eta_{ji,t_l}^{\mathrm{rnd}}\psi_{ji,t_l}^{\mathrm{rnd}}\right]^{\mathsf{T}}$ is the subvector of $\mathbf{e}_{ij}$ corresponding to reporting instant t_l and includes all the corresponding random errors of PMU measurements.

When considering multiple branches simultaneously, problem (6) can be extended to find the vector $\mathbf{x} =$

$\cup_{(i,j)\in\Gamma}\mathbf{x}_{ij}$, namely, the vector of the unknown line parameter deviations and systematic errors for all the considered branches in a set Γ. This is referred to as the multiple-branch approach as opposed to the single-branch approach and it is effective in reducing the estimation error when the considered branches share some nodes [15]. The overall problem, in this case, becomes

$$\mathbf{b} = \begin{bmatrix} \vdots \\ \mathbf{b}_{ij} \\ \vdots \end{bmatrix} = \mathbf{H}\mathbf{x} + \boldsymbol{\epsilon} = \mathbf{H}\mathbf{x} + \mathbf{E}\mathbf{e} = \mathbf{H}\mathbf{x} + \begin{bmatrix} \ddots & & \\ & \mathbf{E}_{ij} & \\ & & \ddots \end{bmatrix} \begin{bmatrix} \vdots \\ \mathbf{e}_{ij} \\ \vdots \end{bmatrix} \tag{7}$$

where $(i,j) \in \Gamma$ and $\mathbf{e}$ is the vector merging all the random vectors $\mathbf{e}_{ij}$. Matrix $\mathbf{H}$ is built from all the matrices $\mathbf{H}_{ij}$ and $\boldsymbol{\epsilon}$ includes all $\boldsymbol{\epsilon}_{ij}$ vectors.

When dealing with multiple branches in the same estimation problem, it is also beneficial to introduce the additional constraints corresponding to zero injection (ZI) nodes where injected current is zero and, thus, Kirchoff's current law can be applied (see [15]). An additional complex equation is thus obtained and, with the above assumptions, the two following linear real-valued equations can be added to (7) for each zero-injection node j:

$$\sum_{h\in\Omega_j} I^r_{jh} = \sum_{h\in\Omega_j} I^r_{jh}\left(\eta^{\text{sys}}_{jh} + \eta^{\text{rnd}}_{jh}\right) - \sum_{h\in\Omega_j} I^x_{jh}\left(\psi^{\text{sys}}_{jh} + \psi^{\text{rnd}}_{jh}\right) \tag{8a}$$

$$\sum_{h\in\Omega_j} I^x_{jh} = \sum_{h\in\Omega_j} I^x_{jh}\left(\eta^{\text{sys}}_{jh} + \eta^{\text{rnd}}_{jh}\right) + \sum_{h\in\Omega_j} I^r_{jh}\left(\psi^{\text{sys}}_{jh} + \psi^{\text{rnd}}_{jh}\right) \tag{8b}$$

where I^r_{jh} and I^x_{jh} are the real and imaginary part of the measured branch current, respectively, and Ω_j is the set of nodes adjacent to node j.

Additional important information for the estimation can be added to (6) and (7) concerning prior knowledge about the unknowns. In fact, variability ranges can be defined for line parameters and, more important, information about IT accuracy can be exploited. For instance, knowing the IT class and nameplate data, it is possible to assume that ξ^{sys}, α^{sys}, η^{sys}, and ψ^{sys} (subscripts are intentionally dropped to indicate the generic node or branch) have prior values and uncertainties.

The easiest prior assumption on all the unknowns is that they are equal to zero (no deviation) with a given random error that depends on the available information. That considered, it is possible to augment (7) as follows:

$$\mathbf{b}_{\text{tot}} = \begin{bmatrix} \mathbf{b} \\ \mathbf{0}_{N\times 1} \end{bmatrix} = \begin{bmatrix} \mathbf{H} \\ \mathbf{I}_N \end{bmatrix}\mathbf{x} + \begin{bmatrix} \boldsymbol{\epsilon} \\ \mathbf{e}_{\text{prior}} \end{bmatrix} = \mathbf{H}_{\text{tot}}\mathbf{x} + \mathbf{e}_{\text{tot}} \tag{9}$$

where N is the size of $\mathbf{x}$, $\mathbf{0}_{N\times 1}$ is the N-size vector of zeros, and $\mathbf{I}_N$ is the N-size identity matrix defining the prior measurement matrix. Finally, $\mathbf{e}_{\text{prior}}$ represents prior errors. The last N rows in (9) are thus associated with the constraints brought by prior knowledge.

The multiple-branch estimation problem (9) (it boils down to the single-branch problem when $\Gamma = \{(i,j)\}$, i.e., a single branch is considered) can be solved via WLS approach. This corresponds to solving the following linear system:

$$\left(\mathbf{H}^{\text{T}}_{\text{tot}}\mathbf{W}_{\text{tot}}\mathbf{H}_{\text{tot}}\right)\hat{\mathbf{x}} = \mathbf{H}^{\text{T}}_{\text{tot}}\mathbf{W}_{\text{tot}}\mathbf{b}_{\text{tot}} \tag{10}$$

that allows computing the vector of the estimates $\hat{\mathbf{x}}$, where $\hat{}$ will indicate the estimated quantities. The weighing matrix is

$$\mathbf{W}_{\text{tot}} = \Sigma^{-1}_{\text{tot}} = \begin{bmatrix} \Sigma_{\boldsymbol{\epsilon}} & \mathbf{0} \\ \mathbf{0} & \Sigma_{\mathbf{e}_{\text{prior}}} \end{bmatrix}^{-1} \tag{11}$$

where $\Sigma_{\boldsymbol{\epsilon}}$ is the covariance matrix of the random vector $\boldsymbol{\epsilon}$ and $\Sigma_{\mathbf{e}_{\text{prior}}}$ is the covariance matrix of prior errors. $\Sigma_{\boldsymbol{\epsilon}}$ can be derived through the law of propagation of uncertainty from the covariance matrix of the random errors $\Sigma_{\mathbf{e}}$ as [29]

$$\Sigma_{\boldsymbol{\epsilon}} = \mathbf{E}\Sigma_{\mathbf{e}}\mathbf{E}^{\text{T}} \tag{12}$$

where $\Sigma_{\mathbf{e}}$ can be filled in using PMU specifications. A common assumption is to consider such a matrix as diagonal since PMU measurements, under many circumstances, can be supposed to be uncorrelated (in particular, when different instruments are considered).

In [15], the main diagonal of matrix $\Sigma_{\mathbf{e}_{\text{prior}}}$ is computed supposing that prior standard deviations of ratio error and phase displacement of both VTs and CTs are the corresponding maximum errors divided by $\sqrt{3}$, thus assuming uniform prior distributions. The same is done for line parameters. This approach is likely to be valid for VTs since voltage magnitude is expected to be rather close to 1 p.u. For CTs, the assumption may be simplistic as discussed in [25]. As for line parameters instead, the robustness of the method to different assumptions about their variability has been already assessed in [30].

For a large number of timestamps, the same approach as in [31] is exploited, namely, (9) is solved as a Tikhonov regularization problem with a tailored regularization term.

B. PROPOSED METHOD

The method summarized in Section III-A does not consider possible variations of η^{sys} and ψ^{sys} across different timestamps. This means that the unknown quantities, for each branch and each measured current, are assumed constant. However, N_t timestamps might correspond to repeated measurements of the same network condition (thanks to the high RR of PMUs) but also to different load conditions (from hereon referred to as cases). When C cases are considered, CT errors depend on I/I^0 and, as discussed in Section II, $\eta^{\text{sys}} = \eta(I/I^0)$ and $\psi^{\text{sys}} = \psi(I/I^0)$ are nonlinear functions.

In this article, we thus propose to change the measurement model to accommodate for variations of the systematic error of a CT depending on the current magnitude. In fact, the more the measurement model reflects the actual behavior of

the CT (condensed by the functions η and ψ), the highest the capability to compensate for systematic errors. Following the same discussion as in Section III-A, (3) (and its counterpart for i_{ji}) changes as follows:

$$i_{ij} = I_{ij}e^{j\theta_{ij}} = \left(1 + \eta_{ij}^{\text{sys}}\left(I_{ij}/I_{ij}^0\right) + \eta_{ij}^{\text{rnd}}\right)I_{ij}^R \cdot \cdot e^{j\left(\theta_{ij}^R + \psi_{ij}^{\text{sys}}\left(I_{ij}/I_{ij}^0\right) + \psi_{ij}^{\text{rnd}}\right)} \tag{13}$$

where $\eta_{ij}^{\text{sys}}()$ and $\psi_{ij}^{\text{sys}}()$ are the ratio and phase error functions of the CT measuring i_{ij} and I_{ij}^0 is the nominal current of the specific CT. Considering the same approximation and linearization performed in Section III-A, from (13), we have

$$i_{ij}^R = I_{ij}^R e^{j\theta_{ij}^R} \simeq I_{ij}e^{j\theta_{ij}}\left[1 - \eta_{ij}^{\text{sys}}\left(I_{ij}/I_{ij}^0\right) - \eta_{ij}^{\text{rnd}} + -j\psi_{ij}^{\text{sys}}\left(I_{ij}/I_{ij}^0\right) - j\psi_{ij}^{\text{rnd}}\right]. \tag{14}$$

The next step is introducing parametric representations for the generic functions $\eta_{ij}^{\text{sys}}()$ and $\psi_{ij}^{\text{sys}}()$, so that their parameters may become additional unknowns in the WLS problem. In principle, adopting a more complex model defined by many parameters would permit to accurately track the actual trends. However, this choice significantly decreases the constraints/unknowns ratio, which is still fairly low as discussed in Section III-A. Furthermore, increasing the number of parameters is likely to lead to overfitting problems that undermine the robustness of the estimates. For this reason, analyzing the shapes of the experimental curves reported in Figs. 2 and 3, we first propose to approximate $\eta_{ij}^{\text{sys}}()$ and $\psi_{ij}^{\text{sys}}()$ as piecewise linear functions, defined by just two parameters each. In particular, the following expressions are considered for the generic timestamp t (symbol $\tilde{}$ indicates the approximate error model):

$$\tilde{\eta}_{ij}^{\text{sys}}\left(\frac{I_{ij,t}}{I_{ij}^0}\right) = \begin{cases} \eta_{ij,\bar{\kappa}_{ij}\%} + m_{\eta,ij}\left(\frac{\bar{\kappa}_{ij}}{100} - \frac{I_{ij,t}}{I_{ij}^0}\right), & \text{if } \frac{\underline{\kappa}_{ij}}{100}I_{ij}^0 < I_{ij,t} < \frac{\bar{\kappa}_{ij}}{100}I_{ij}^0 \\ \eta_{ij,\bar{\kappa}_{ij}\%}, & \text{if } I_{ij,t} \geq \frac{\bar{\kappa}_{ij}}{100}I_{ij}^0 \end{cases} \tag{15}$$

$$\tilde{\psi}_{ij}^{\text{sys}}\left(\frac{I_{ij,t}}{I_{ij}^0}\right) = \begin{cases} \psi_{ij,\bar{\lambda}_{ij}\%} + m_{\psi,ij}\left(\frac{\bar{\lambda}_{ij}}{100} - \frac{I_{ij,t}}{I_{ij}^0}\right), & \text{if } \frac{\underline{\lambda}_{ij}}{100}I_{ij}^0 < I_{ij,t} < \frac{\bar{\lambda}_{ij}}{100}I_{ij}^0 \\ \psi_{ij,\bar{\lambda}_{ij}\%}, & \text{if } I_{ij,t} \geq \frac{\bar{\lambda}_{ij}}{100}I_{ij}^0 \end{cases} \tag{16}$$

where $\eta_{ij,\bar{\kappa}_{ij}\%}$ and $\psi_{ij,\bar{\lambda}_{ij}\%}$ represent, respectively, the systematic ratio error and phase displacement at $\bar{\kappa}_{ij}\%$ and $\bar{\lambda}_{ij}\%$ of the nominal current (e.g., $I_{ij,t}/I_{ij}^0 = \bar{\lambda}_{ij}/100$) for the considered CT. The model is thus composed of two regions: 1) for low current ($\underline{\kappa}_{ij}/100$ is the lowest considered current ratio for magnitude errors while $\underline{\lambda}_{ij}/100$ is that associated with phase displacement), we have a linear trend with slope $m_{\eta,ij}$ (or $m_{\psi,ij}$ for phase displacement) and 2) for high current ($\bar{\kappa}_{ij}/100$, or $\bar{\lambda}_{ij}/100$, is the ratio of the function knee), we have a horizontal line. The proposed model can be included in the estimation by replacing (15) and (16) into (14), (14) into (4) and (5), and then following the same steps as in Section III-A with the appropriate changes. In particular, the vector of unknowns $\mathbf{x}_{ij}$ in (6) is replaced with

$$\mathbf{x}'_{ij} = \begin{bmatrix} \xi_i^{\text{sys}} \\ \alpha_i^{\text{sys}} \\ \xi_j^{\text{sys}} \\ \alpha_j^{\text{sys}} \\ \eta_{ij,\bar{\kappa}_{ij}\%} \\ m_{\eta,ij} \\ \psi_{ij,\bar{\lambda}_{ij}\%} \\ m_{\psi,ij} \\ \eta_{ji,\bar{\kappa}_{ji}\%} \\ m_{\eta,ji} \\ \psi_{ji,\bar{\lambda}_{ji}\%} \\ m_{\psi,ji} \\ \gamma_{ij} \\ \beta_{ij} \\ \delta_{ij} \end{bmatrix} \tag{17}$$

where two unknowns are added for each current measurement. This allows the flexibility to deal with nonconstant systematic errors across cases. With the new method, the parameters of the piecewise linear error functions are thus to be estimated through the new problem defined by

$$\mathbf{b}_{ij} = \mathbf{H}'_{ij}\mathbf{x}'_{ij} + \boldsymbol{\epsilon}_{ij} = \mathbf{H}'_{ij}\mathbf{x}'_{ij} + \mathbf{E}_{ij}\mathbf{e}_{ij} \tag{18}$$

where $\mathbf{H}'_{ij}$ is the new measurement matrix and it is obtained using for $\eta_{ij,\bar{\kappa}_{ij}\%}$, $\eta_{ji,\bar{\kappa}_{ji}\%}$, $\psi_{ij,\bar{\lambda}_{ij}\%}$, and $\psi_{ji,\bar{\lambda}_{ji}\%}$ the same columns associated in $\mathbf{H}_{ij}$ with η_{ij}^{sys}, η_{ji}^{sys}, ψ_{ij}^{sys}, and ψ_{ji}^{sys}, respectively, and multiplying those columns by suitable factors to obtain the corresponding columns for $m_{\eta,ij}$, $m_{\eta,ji}$, $m_{\psi,ij}$, and $m_{\psi,ji}$ (e.g., $\bar{\kappa}_{ij}/100 - I_{ij}/I_{ij}^0$ for $m_{\eta,ij}$).

Following the same approach, it is also possible to integrate multiple branches in the estimator, defining a problem in the form (7). More complex is instead the inclusion of prior information. As in (9), all unknowns can be assumed to be zero with a given uncertainty. Supposing that $m_{\eta,ij}$ and $m_{\psi,ij}$ are zero (for all branches) means that the prior error function for each CT (for both ratio error and phase displacement) is constant regardless the current level. $\boldsymbol{\Sigma}_{\mathbf{e}_{\text{prior}}}$ is defined as in Section III-A for all the unknowns but those related to CTs. Prior standard deviation of $\eta_{ij,\bar{\kappa}_{ij}\%}$ is obtained from the CT class specifications; in particular, in the tests, $\bar{\kappa}_{ij} = 100$ is considered for all the branches. This means that, assuming a uniform prior distribution, the prior standard deviation of $\eta_{ij,\bar{\kappa}_{ij}\%}$ corresponds to the CT accuracy class divided by $\sqrt{3}$. Similar assumptions are made for $\psi_{ij,\bar{\lambda}_{ij}\%}$ and for the opposite current direction. Concerning the slope parameter, e.g., $m_{\eta,ij}$, its range can be found for a given $\bar{\kappa}_{ij}$ (which is a configuration parameter of the algorithm) considering all the ratio error curves that can be defined for every

value of $\eta_{ij,\bar{\kappa}_{ij}\%}$ and do not violate the limits of the class. Each curve is characterized by a slope value and, thus, the prior interval can be defined as the range spanned by these values. Also in this case, uniform distribution is assumed in the absence of additional information. A similar procedure is adopted for phase displacement. It is important to recall that $\Sigma_{\mathbf{e}_{\text{prior}}}$ contributes to the computation of the weighing matrix; thus, it does not add a stiff constraint on the unknowns, but it helps in narrowing the ranges of their possible values according to available prior information. Once $\Sigma_{\mathbf{e}_{\text{prior}}}$ is filled in ($\Sigma_{\boldsymbol{\epsilon}}$ is the same as before), the analogous of (9) and (11) can be written and the analogous of (10) can be solved to find the estimated vector $\hat{\mathbf{x}}'$.

Once the estimates are available, focusing on the CT measuring current i_{ij}, it is possible to obtain also its systematic errors for all the timestamps $t_1, \ldots, t_{N_t}$ as

$$\hat{\eta}_{ij}^{\text{sys}} = \hat{\eta}_{ij,\bar{\kappa}_{ij}\%} + \hat{m}_{\eta,ij}\left(\frac{\bar{\kappa}_{ij}}{100} - \frac{I_{ij,t_l}}{I_{ij}^0}\right) \tag{19}$$

$$\hat{\psi}_{ij}^{\text{sys}} = \hat{\psi}_{ij,\bar{\lambda}_{ij}\%} + \hat{m}_{\psi,ij}\left(\frac{\bar{\lambda}_{ij}}{100} - \frac{I_{ij,t_l}}{I_{ij}^0}\right). \tag{20}$$

This method, which will be referred to as DynCTlin in the following, is based on a model of the CT that deals with the variations of the currents across cases and on piecewise linear error functions. Another possibility is here proposed, that is using a nonlinear approximation of the error function. It is important to highlight that the number of additional unknowns needs to be concise to avoid overfitting and ill conditioning; thus, the following expressions are proposed:

$$\tilde{\eta}_{ij}^{\text{sys}}\left(\frac{I_{ij,t}}{I_{ij}^0}\right) = \begin{cases} \eta_{ij,\bar{\kappa}_{ij}\%} + m_{\eta,ij}\left(\frac{\bar{\kappa}_{ij}}{100} - \frac{I_{ij,t}}{I_{ij}^0}\right)^{\chi}, & \text{if } \frac{\kappa_{ij}}{100} I_{ij}^0 < I_{ij,t} < \frac{\bar{\kappa}_{ij}}{100} I_{ij}^0 \\ \eta_{ij,\bar{\kappa}_{ij}\%}, & \text{if } I_{ij,t} \geq \frac{\bar{\kappa}_{ij}}{100} I_{ij}^0 \end{cases} \tag{21}$$

$$\tilde{\psi}_{ij}^{\text{sys}}\left(\frac{I_{ij,t}}{I_{ij}^0}\right) = \begin{cases} \psi_{ij,\bar{\lambda}_{ij}\%} + m_{\psi,ij}\left(\frac{\bar{\lambda}_{ij}}{100} - \frac{I_{ij,t}}{I_{ij}^0}\right)^{\chi}, & \text{if } \frac{\lambda_{ij}}{100} I_{ij}^0 < I_{ij,t} < \frac{\bar{\lambda}_{ij}}{100} I_{ij}^0 \\ \psi_{ij,\bar{\lambda}_{ij}\%}, & \text{if } I_{ij,t} \geq \frac{\bar{\lambda}_{ij}}{100} I_{ij}^0 \end{cases} \tag{22}$$

to replace (15) and (16), respectively, using only two parameters as in the previous case. A possible choice for χ, according to the error trends reported in Section II, is 2. All the steps in the definition of this new version of the estimation method (DynCTsquare) are the same as DynCTlin, with the definition of new measurement and weighing matrices.

IV. TESTS AND RESULTS

Tests are performed through simulations on the 15-kV test network shown in Fig. 5 (reporting node and branch indices),

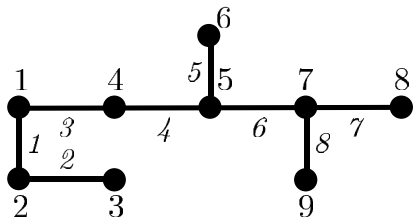

FIGURE 5. Test network.

TABLE 1. Nominal line parameters of the test network.

Branch	R_{ij}^0 [p.u.]	X_{ij}^0 [p.u.]	$B_{sh,ij}^0$ [p.u.]
1	0.055	0.057	0.00017
2	0.039	0.12	0.00065
3	0.049	0.051	0.00015
4	0.098	0.33	0.0016
5	0.17	0.066	0.00012
6	0.21	0.20	0.00066
7	0.24	0.09	0.00017
8	0.26	0.18	0.00048

TABLE 2. Active and reactive power of the loads.

Node	P_h [MW]	Q_h [Mvar]
2	0	0
3	3.28	0.57
4	0	0
5	0	0
6	0.12	0.017
7	0	0
8	0.24	0.035
9	4	4

which represents a portion of a larger DS. Resistance, reactance, and transversal susceptance values have been obtained using typical *per length* values for DS line cables. The nominal values of line parameters are reported in Table 1. The active and reactive powers shown in Table 2 are assumed as nominal values for the absorbed power at each node. A DG plant connected to node 9 has been also considered.

The tests are carried out considering all the branches of the grid and different operating conditions, in order to assess the performance of the algorithm with several values of I_{ij}^R/I_{ij}^0 or I_{ji}^R/I_{ji}^0, leading to different CT errors. $I^0{}_{ij}$ represents the rated primary current of the CT that measures i_{ij}.

Each test involves $N_{\text{MC}} = 5000$ Monte Carlo (MC) trials used to evaluate the root mean square errors (RMSEs) of the estimated quantities. A trial corresponds to a given random extraction of the line parameters. The estimation model is based on $N_t = 10C$ timestamps, corresponding to C different load configurations (cases) of the network and ten reporting instants for each condition (the latter can be considered a conservative configuration). $C = 200$ has been considered for all the tests. The reference values of voltages and currents in

each condition are obtained from a powerflow computation and then corrupted with measurement errors. In particular, the tests are prepared according to the following assumptions.

1) Line parameters, i.e., R_{ij}, X_{ij}, and $B_{sh,ij}$, vary from nominal values in a $\pm 15\,\%$[2] range with uniform distribution across MC trials.
2) ITs belong to class 0.5. For VTs, 0.5 % and 0.6 crad are the maximum ratio error and phase displacement and, for each MC trial, the errors are extracted from uniform distributions. The superimposed CT errors are instead extracted, for each MC trial, considering current measurement and CT type, starting from the corresponding error functions of Figs. 2 and 3 (see Section II). In particular, considering the class limits at different current magnitude levels, the maximum scaling factor that allows amplifying the error resulting from the corresponding function without violating class prescriptions is computed for both magnitude (ν_{mag}) and phase-angle (ν_{ph}). Then, for every MC trial, two uniform random variables μ_{mag} and $\mu_{\text{ph}} \in [-1, 1]$ are extracted for magnitude and phase-angle, respectively. For a given timestamp and current I_{ij}^R, the resulting systematic errors are thus

$$\eta_{ij}^{\text{sys}} = \mu_{\text{mag}} \nu_{\text{mag}} \, \eta\left(\frac{I_{ij}^R}{I_{ij}^0}\right) \tag{23}$$

$$\psi_{ij}^{\text{sys}} = \mu_{\text{ph}} \nu_{\text{ph}} \, \psi\left(\frac{I_{ij}^R}{I_{ij}^0}\right). \tag{24}$$

3) Two PMU accuracy levels are assumed. The first one, called "PMU01," has maximum magnitude error of 0.1% and maximum phase-angle error of 0.1 crad. The second one, "PMU02," has double error limits for both magnitude and phase. All the errors are assumed as uniformly distributed, which represents a conservative hypothesis.
4) Starting from the base case, load and generator powers have been scattered within ±10% among the 200 different cases of each MC trial using random extractions from uniform distributions.

RMSE values across MC trials are used to assess the estimation performance for line parameters, whereas, for the estimates of CT systematic errors, RMSEs are computed with respect to both cases and MC trials since we have different parameters for each case.

Figs. 6 and 7 compare the estimation results for magnitude and phase CT errors obtained with the method in [25] (indicated as "Static") and the proposed methods DynCTlin and DynCTsquare (indicated in the figures with red, blue and black colors, respectively) considering CT1 (see Figs. 2 and 3, dashed line). The comparison has been evaluated with and without ZI constraints (denoted with stars and squares, respectively).

2. In the literature (e.g., [2], [15], [28], and [32]), line parameter deviations up to tens of percent are considered; in this work 15 % is adopted.

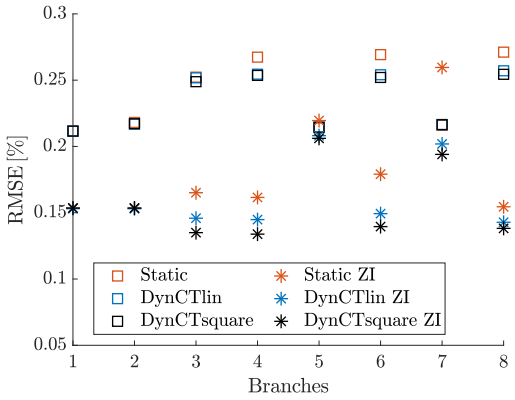

FIGURE 6. Comparison of η^{sys} estimation results (PMU01 and $C = 200$).

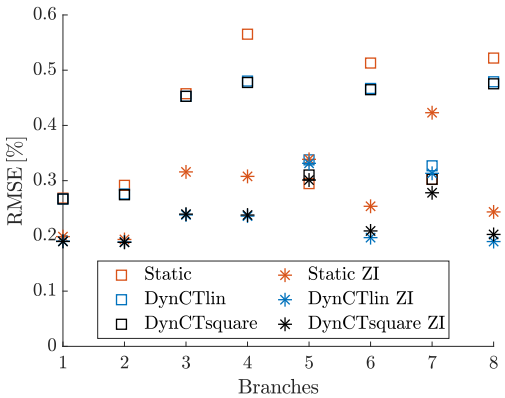

FIGURE 7. Comparison of ψ^{sys} estimation results (PMU01 and $C = 200$).

It is possible to highlight two aspects. The first one is that ZI constraints have enabled to halve the CT errors estimates with respect to those obtained without these constraints for all three methods. The second is that the estimation results of the proposed methods (DynCTlin and DynCTsquare) are better than those obtained with Static for both magnitude and phase. Basically, for all the branches, the refined estimation model of CT behavior permits estimating CT errors more accurately.

Other tests have been then carried out in order to evaluate the benefits obtained by the proposed methods in the estimation of the line parameters. In particular, the results relevant to transversal susceptance estimations are particularly meaningful. Fig. 8 shows a comparison of δ estimation RMSEs (the branch index k shown in Fig. 5 is used to simplify the notation) obtained introducing ZI constraints. Also in this case, CT1 has been considered. These estimation results must then be compared with the prior standard deviation of the line parameters, i.e., $\Delta_\gamma = \Delta_\beta = \Delta_\delta = 15/\sqrt{3} = 8.66\%$.

It is worth highlighting that the method that considers a static model for CT errors (indicated in Fig. 8 with red squares) has RMSEs, for branches 1, 2, 3, and 8, which are higher than the prior standard deviation. For the same branches, the methods DynCTlin and DynCTsquare

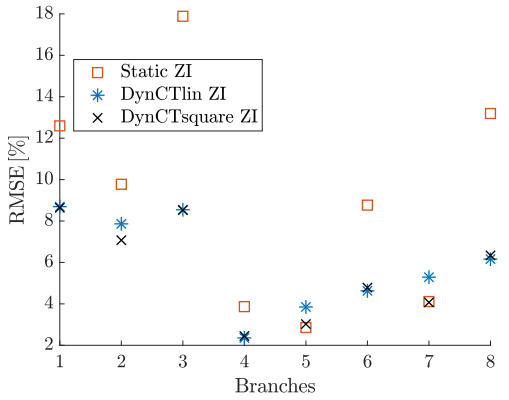

FIGURE 8. Comparison of δ estimation results (PMU01 and $C = 200$).

TABLE 3. Comparison of γ and β estimations (ZIs are used).

Method	PMU Accuracy	RMSE [%]					
		γ_{45} [%]	β_{45} [%]	γ_{57} [%]	β_{57} [%]	γ_{79} [%]	β_{79} [%]
Static	PMU01	7.70	3.85	5.60	6.16	6.23	7.35
	PMU02	8.31	6.04	7.33	7.64	7.79	8.29
DynCTlin	PMU01	7.59	3.62	5.34	5.91	5.96	7.16
DynCTsquare	PMU02	8.27	5.79	7.17	7.52	7.67	8.22

TABLE 4. Performance comparison in the presence of different PMU and CT configurations (ZIs are used).

CT	PMU	Method	RMSE					
			δ_{45} [%]	η_{45}^{sys} [%]	ψ_{45}^{sys} [crad]	δ_{79} [%]	η_{79}^{sys} [%]	ψ_{79}^{sys} [crad]
CT1	PMU01	Static	3.87	0.16	0.31	13.19	0.15	0.24
		DynCTlin	2.36	0.14	0.24	6.16	0.14	0.19
		DynCTsquare	2.45	0.13	0.24	6.34	0.14	0.20
	PMU02	Static	3.67	0.15	0.27	9.69	0.15	0.24
		DynCTlin	2.65	0.15	0.25	6.86	0.15	0.21
		DynCTsquare	2.79	0.14	0.25	6.96	0.15	0.22
CT2	PMU01	Static	4.49	0.18	0.34	15.28	0.16	0.26
		DynCTlin	2.89	0.16	0.25	6.95	0.15	0.19
		DynCTsquare	2.83	0.14	0.24	6.67	0.14	0.20
	PMU02	Static	4.17	0.16	0.28	10.74	0.16	0.24
		DynCTlin	3.15	0.16	0.26	7.33	0.16	0.21
		DynCTsquare	3.14	0.15	0.25	7.18	0.15	0.22
CT3	PMU01	Static	3.27	0.15	0.29	11.17	0.15	0.24
		DynCTlin	1.84	0.14	0.23	5.52	0.14	0.19
		DynCTsquare	2.15	0.13	0.24	6.13	0.14	0.21
	PMU02	Static	3.23	0.15	0.27	8.79	0.15	0.25
		DynCTlin	2.20	0.14	0.24	6.50	0.16	0.22
		DynCTsquare	2.53	0.14	0.25	6.82	0.15	0.23

(indicated with blue stars and black cross, respectively) ensure estimates below Δ_δ; more specifically, for branch 8, the improvement is about 29% of the prior standard deviation. The maximum improvement reached with respect to Δ_δ is of about 72% for branch 4. Notwithstanding the noticeable improvement, it is clear that achieving RMSE below a few percent is still difficult. This highlights once more that the estimation task, under realistic conditions, is challenging. It can be partially addressed by using a higher number of measurements and possibly more accurate PMUs.

Table 3 shows the comparison for γ and β estimations with the same type of CT used in the previous tests and with PMU01 and PMU02 accuracy levels. The results confirm the conclusion drawn in [25] on the fact that longitudinal parameters are not significantly affected by the presence of CT errors that are not constant across the limited load variations considered in the cases. DynCTlin and DynCTsquare methods have basically identical behavior, and Static has slightly worse results. For all of them, with low PMU accuracy, the parameter estimations degrade significantly, but RMSEs still remain below the prior standard deviations Δ_γ and Δ_β.

Finally, for the sake of a comprehensive investigation about the behavior of the proposed approach, Table 4 reports for two branches the estimation results of CT errors and shunt susceptances, with different PMU accuracies and for all the three CT types presented in Section II. The systematic errors are extracted from the corresponding curves (dashed line CT1, dashed line CT2, solid line CT3) in Figs. 2 and 3. It is possible to observe that the complex behavior of the CTs has negative impact on the Static approach, as already observed in [25]. The proposed dynamic methods overcome the problem achieving good estimations with slight differences between them, due to the different approximations introduced to model CT behavior. In particular, DynCTlin is slightly better for CT1 and CT3, while DynCTsquare is marginally better for CT2. A possible explanation of this behavior can be obtained observing Fig. 3, focusing on the low I/I^0 region, since the error function of CT2 appears steeper than those of CT1 and CT3 and, thus, it is better matched with a nonlinear representation.

Focusing on η^{sys} and ψ^{sys} estimation results, the impact of CTs is larger on phase displacement estimation than on ratio error. This is probably due to the wider phase-displacement variation of CTs, as from Figs. 2 and 3. The estimates of η^{sys} and ψ^{sys} are, even in the worst PMU accuracy scenario, more than halved with respect to the prior standard deviation associated with the actual operating conditions (i.e., the actual current ratio) and the estimates obtained with adaptive methods are always equal or better than those achieved with the Static representation. As a final comment, it is also possible to underline that, as in [25], a better PMU accuracy (PMU01) leads to higher RMSEs as the Static approach

is adopted, since it imposes stricter constraints that, in the presence of a model mismatch, can be harmful.

V. CONCLUSION

This article has proposed a new approach to PMU-based line parameter estimation and compensation of the systematic error introduced by CTs. A detailed modeling of the transformer behavior under different operating conditions allows systematic errors to be better represented, thus improving the estimation. In particular, CTs have a relevant impact on shunt susceptance estimation and the proposed algorithms try to fill the gap between CT behavior and method assumptions. In this way, the estimation of CT magnitude error and phase displacement is also remarkably enhanced.

Future developments can concern the investigation of the impact of different types of loads and generators (e.g., capacitors banks, charging stations, etc.) and the generalization to three-phase systems, also considering possible correlations in the parameters. Another challenging topic is the exploitation of conventional measurements to complement the estimation; however, the lack of synchronization or accurate timestamping requires ad hoc treatment and can limit the actual informative content brought by these measurements.

REFERENCES

[1] V. L. Srinivas and J. Wu, "Topology and parameter identification of distribution network using smart meter and μPMU measurements," *IEEE Trans. Instrum. Meas.*, vol. 71, pp. 1–14, 2022.

[2] M. Asprou and E. Kyriakides, "Identification and estimation of erroneous transmission line parameters using PMU measurements," *IEEE Trans. Power Del.*, vol. 32, no. 6, pp. 2510–2519, Dec. 2017.

[3] A. Monti, C. Muscas, and F. Ponci, Eds., *Phasor Measurement Units and Wide Area Monitoring Systems*, 1st ed. London, U.K.: Academic, 2016.

[4] A. von Meier, E. Stewart, A. McEachern, M. Andersen, and L. Mehrmanesh, "Precision micro-synchrophasors for distribution systems: A summary of applications," *IEEE Trans. Smart Grid*, vol. 8, no. 6, pp. 2926–2936, Nov. 2017.

[5] M. R. Rezaei, S. R. Hadian-Amrei, and M. R. Miveh, "Online identification of power transformer and transmission line parameters using synchronized voltage and current phasors," *Electr. Power Syst. Res.*, vol. 203, pp. 1–10, Feb. 2022.

[6] H. Goklani, G. Gajjar, and S. A. Soman, "Quantification of minimum unbalance required for accurate estimation of sequence parameters of transmission line using PMU data," in *Proc. IEEE Power Energy Soc. Gen. Meeting (PESGM)*, Atlanta, GA, USA, Aug. 2019, pp. 1–5.

[7] V. Milojević, S. Čalija, G. Rietveld, M. V. Ačanski, and D. Colangelo, "Utilization of PMU measurements for three-phase line parameter estimation in power systems," *IEEE Trans. Instrum. Meas.*, vol. 67, pp. 2453–2462, 2018.

[8] J. Sun, M. Xia, and Q. Chen, "A classification identification method based on phasor measurement for distribution line parameter identification under insufficient measurements conditions," *IEEE Access*, vol. 7, pp. 158732–158743, 2019.

[9] Y. Hou, T. Fang, F. Shi, and H. Zhang, "Parameter estimation method of distribution network based on PMU measurement data," in *Proc. 5th Asia Conf. Power Electr. Eng. (ACPEE)*, 2020, pp. 1620–1625.

[10] Y. Wang, M. Xia, Q. Yang, Y. Song, Q. Chen, and Y. Chen, "Augmented state estimation of line parameters in active power distribution systems with phasor measurement units," *IEEE Trans. Power Del.*, vol. 37, no. 5, pp. 3835–3845, Oct. 2022.

[11] M. Xiao et al., "Distribution line parameter estimation driven by probabilistic data fusion of D-PMU and AMI," *IET Gener. Transm. Distrib.*, vol. 15, no. 20, pp. 2883–2892, 2021.

[12] R. K. Gupta, F. Sossan, J.-Y. Le Boudec, and M. Paolone, "Compound admittance matrix estimation of three-phase untransposed power distribution grids using synchrophasor measurements," *IEEE Trans. Instrum. Meas.*, vol. 70, pp. 1–13, 2021.

[13] C. M. Roberts, C. M. Shand, K. W. Brady, E. M. Stewart, A. W. McMorran, and G. A. Taylor, "Improving distribution network model accuracy using impedance estimation from micro-synchrophasor data," in *Proc. PES Gen. Meeting (PESGM)*, 2016, pp. 1–5.

[14] A. Mingotti, L. Peretto, R. Tinarelli, A. Angioni, A. Monti, and F. Ponci, "Calibration of synchronized measurement system: From the instrument transformer to the PMU," in *Proc. IEEE 9th Int. Workshop Appl. Meas. Power Syst. (AMPS)*, 2018, pp. 1–5.

[15] P. A. Pegoraro, K. Brady, P. Castello, C. Muscas, and A. von Meier, "Line impedance estimation based on synchrophasor measurements for power distribution systems," *IEEE Trans. Instrum. Meas.*, vol. 68, pp. 1002–1013, 2019.

[16] *Instrument Transformers—Part 1: General Requirements*, Standard IEC 61869-1:2009, 2009.

[17] D. Carta, A. Benigni, C. Sitzia, P. A. Pegoraro, and S. Sulis, "Performance assessment of synchronized phasor measurement-based parameter estimation for distribution networks," in *Proc. Int. Conf. Smart Energy Syst. Technol. (SEST)*, Sep. 2022, pp. 1–6.

[18] CENELEC, *Voltage Characteristics of Electricity Supplied by Public Electricity Networks*, European Standard EN50160:2010+A3, 2019.

[19] *Instrument Transformers—Part 3: Additional Requirements for Inductive Voltage Transformers*, Standard IEC 61869-3:2011, 2017.

[20] *Instrument Transformers—Part 11: Additional Requirements for Low-Power Passive Voltage Transformers*, Standard IEC 61869-11:2017, 2017.

[21] C. Laurano, S. Toscani, and M. Zanoni, "A simple method for compensating harmonic distortion in current transformers: Experimental validation," *Sensors*, vol. 21, no. 9, p. 2907, 2021.

[22] M. Faifer, C. Laurano, R. Ottoboni, and S. Toscani, "Compensating the harmonic distortion introduced by instrument transformers: An improved method based on frequency-domain polynomials," in *Proc. IEEE 11th Int. Workshop Appl. Meas. Power Syst. (AMPS)*, 2021, pp. 1–6.

[23] *Instrument Transformers—Part 2: Additional Requirements for Current Transformers*, Standard IEC 61869-2-:2012, 2012.

[24] *Instrument Transformers—Part 10: Additional Requirements for Low-Power Passive Current Transformers*, Standard IEC 61869-10:2017, 2017.

[25] C. Sitzia, P. A. Pegoraro, A. V. Solinas, S. Sulis, C. Laurano, and S. Toscani, "Impact of current transformers on line parameters estimation based on synchronized measurements," in *Proc. IEEE 12th Int. Workshop Appl. Meas. Power Syst. (AMPS)*, Sep. 2022, pp. 1–6.

[26] A. Mingotti, L. Peretto, L. Bartolomei, D. Cavaliere, and R. Tinarelli, "Are inductive current transformers performance really affected by actual distorted network conditions? An experimental case study," *Sensors*, vol. 20, no. 3, p. 927, 2020.

[27] R. Pintelon and J. Schoukens, *System Identification: A Frequency Domain Approach*. Hoboken, NJ, USA: Wiley, 2012.

[28] P. A. Pegoraro, K. Brady, P. Castello, C. Muscas, and A. von Meier, "Compensation of systematic measurement errors in a PMU-based monitoring system for electric distribution grids," *IEEE Trans. Instrum. Meas.*, vol. 68, pp. 3871–3882, 2019.

[29] "Evaluation of data—Guide to the expression of uncertainty in measurement," BIPM, Sèvres, France, document JCGM 100:2008, Sep. 2008.

[30] C. Muscas et al., "Characterization of a PMU-based method for transmission line parameters estimation with systematic measurement error modeling," in *Proc. AEIT Int. Annu. Conf.*, 2021, pp. 1–6.

[31] C. Sitzia, C. Muscas, P. A. Pegoraro, A. V. Solinas, and S. Sulis, "Enhanced PMU-based line parameters estimation and compensation of systematic measurement errors in power grids considering multiple operating conditions," *IEEE Trans. Instrum. Meas.*, vol. 71, pp. 1–12, 2022.

[32] G. L. Kusic and D. L. Garrison, "Measurement of transmission line parameters from SCADA data," in *Proc. IEEE PES Power Syst. Conf. Expo.*, Oct. 2004, pp. 344–349.

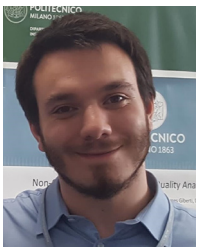

CHRISTIAN LAURANO (Member, IEEE) received the M.S. and Ph.D. degrees (*cum laude*) in electrical engineering from the Politecnico di Milano, Milan, Italy, in 2014 and 2018, respectively.

He was a Postdoctoral Researcher with the Politecnico di Milano from 2018 to 2020. He was with the Measurement and Diagnostic Group, Transmission and Distribution Technology Department, RSE SpA, Milan, from 2020 to 2021. He is currently an Assistant Professor with the Dipartimento di Elettronica, Informazione e Bioingegneria, Politecnico di Milano. His main research interests include innovative methods to model and characterize electrical transducers, diagnostic techniques devoted to electrical grid components, and power quality monitoring.

PAOLO ATTILIO PEGORARO (Senior Member, IEEE) received the M.S. (*summa cum laude*) degree in telecommunication engineering and the Ph.D. degree in electronic and telecommunication engineering from the University of Padua, Padua, Italy, in 2001 and 2005, respectively.

He was an Assistant Professor with the Department of Electrical and Electronic Engineering, University of Cagliari, Cagliari, Italy, from 2015 to 2018, where he is currently an Associate Professor. He has authored or coauthored over 140 scientific papers. His current research interests include the development of new measurement techniques for modern power networks, with attention to synchronized measurements and state estimation.

Dr. Pegoraro is a member of IEEE IMS TC 39 "Measurements in Power Systems" and of IEC TC 38/WG 47. He is an Associate Editor of the IEEE TRANSACTIONS ON INSTRUMENTATION AND MEASUREMENT and the General Chair of the IEEE International Workshop on Applied Measurements for Power Systems.

CARLO SITZIA (Graduate Student Member, IEEE) received the M.S. degree (*cum laude*) in electrical engineering from the University of Cagliari, Cagliari, Italy, in 2020, where he is currently pursuing the Ph.D. degree with the Electrical and Electronic Measurements Group, Department of Electrical and Electronic Engineering.

His research activities focus on parameter estimation for modern power networks, phasor measurements, and instrument transformers.

ANTONIO VINCENZO SOLINAS (Member, IEEE) received the M.S. degree in electronic engineering and the Ph.D. degree in industrial engineering from the University of Cagliari, Cagliari, Italy, in 2000 and 2022, respectively.

He worked for about 20 years as an R&D Manager on audio and video acquisition, compression and transmission over IP. He is currently a Postdoctoral Research Fellow with the Electrical and Electronic Measurements Group, Department of Electrical and Electronic Engineering, University of Cagliari. He has coauthored more than ten scientific articles published in international journals and conference proceedings. His main research interests include optimization techniques for estimation and monitoring in power systems with attention to synchronized measurements.

SARA SULIS (Senior Member, IEEE) received the M.S. degree in electrical engineering and the Ph.D. degree in industrial engineering from the University of Cagliari, Cagliari, Italy, in 2002 and 2006, respectively.

She is currently an Associate Professor of Electrical and Electronic Measurements with the University of Cagliari. She has authored or coauthored more than 120 scientific articles. Her current research interests include distributed measurement systems designed to perform state estimation and harmonic source estimation of distribution networks.

Dr. Sulis is a member of the Instrumentation and Measurement Society, IEEE TC 39 "Measurements in Power Systems," and CENELEC TC 38 "Instrument Transformers." She is an Associate Editor of the IEEE TRANSACTIONS ON INSTRUMENTATION AND MEASUREMENT and a Power Quality Topic Editor for journals *Energies*, *Applied Sciences*, *Electronics*, and *Sensors*.

SERGIO TOSCANI (Senior Member, IEEE) received the M.S. (*summa cum laude*) and the Ph.D. (*summa cum laude*) degrees in electrical engineering from the Politecnico di Milano, Italy, in 2007 and 2011, respectively.

He was an Assistant Professor of Electrical and Electronic Measurement with the Dipartimento di Elettronica, Informazione e Bioingegneria, Politecnico di Milano from 2011 to 2020, where he currently serves as an Associate Professor. His research activity is mainly focused on development and testing of current and voltage transducers, measurement techniques for power systems, electrical components, and system diagnostics.

Dr. Toscani is a member of the IEEE Instrumentation and Measurement Society and IEEE TC 39 "Measurements in Power Systems".

Open Access funding provided by 'Università degli Studi di Cagliari' within the CRUI CARE Agreement